Q-Factor Measurement with Network Analyzer

DARKO KAJFEZ, SENIOR MEMBER, IEEE, AND EUGENE J. HWAN, MEMBER IEEE

Abstract—Ginzton's impedance method of Q-factor measurement is adapted to network analyzer techniques. The circuit model of the resonator incorporates also an external reactance which varies linearly with frequency to take into account the effects of the coupling mechanism and the influence of the distant resonant modes.

I. Introduction

THE RESONANT microwave circuits, such as microstrip transmission lines or dielectric resonators, exhibit sharp resonances at distinct frequencies. In the vicinity of each resonance, the behavior of the resonator may be described by an equivalent lumped resonant circuit. The three basic parameters of the equivalent resonant circuit are: the unloaded resonant frequency f_0, the unloaded Q factor Q_0, and the coupling factor κ.

The input impedance as a function of frequency of a typical resonator describes a nearly perfect circle. Ginzton [1] describes in detail the analysis of measured circles on the Smith chart in order to deduce the values of Q_0 and κ. The procedure described by Ginzton was developed at the time when impedances were measured with the use of slotted lines. It was then appropriate to define the "detuned short" and "detuned open" reference points on the slotted line, and to interpret the data with respect to one or the other of these two points. The implied assumption was that the reactance X_e of the external circuit can be neglected.

Nowadays, the impedance is measured much faster with the network analyzer [2]. The reference plane of such a measurement coincides with the end of transmission line leading to the resonator, while the "detuned short" or "detuned open" points are difficult to locate and of no advantage in interpreting the data. The procedure to be described here uses the data directly, such as shown on the polar display of the network analyzer. Furthermore, the analysis which follows does not require that the reactance of the external circuit be negligible.

In the measurement method to be described, the resonator is located at the end of the transmission line which leads to the network analyzer. A recent paper [3] has described an alternative method in which the resonator is coupled to the doubly-terminated transmission line like a bandstop filter. Each of these methods should find its use in different circuit configurations.

II. Circuit Model

The equivalent circuit for the input impedance Z_i of an inductance-coupled cavity is shown in Fig. 1(a). The circuit is of the Foster type, consisting of an infinite number of parallel resonant circuits, one for each resonant mode in the cavity [4]. If the cavity was capacitance-coupled, the inductance L_s would have to be replaced by a capacitance. The transmission line of the characteristic impedance R_c (a real number) to the left of the input terminals represents the cable leading to the network analyzer.

The measurement is performed in the narrow range of frequencies around the value ω_0, the resonant frequency under observation. In this narrow range of frequencies, the remainder of the circuit in Fig. 1(a) is replaced by an equivalent "external" impedance $R_e + jX_e$ as shown in Fig. 1(b). For the sake of simplicity, R_e will be neglected and X_e will be presented by the first two terms of a Taylor series

$$X_e = X_1 + 2R_cQ_1\delta. \tag{1}$$

The constant part is denoted by X_1, and the slope of the linearly growing part is denoted by $2Q_1$. The frequency detuning parameter δ is defined as follows

$$\delta = \frac{\omega - \omega_0}{\omega_0}. \tag{2}$$

The input impedance measured by the network analyzer is then

$$Z_i = jX_e + \frac{R_0}{1 + jQ_0\left(\frac{\omega}{\omega_0} - \frac{\omega_0}{\omega}\right)}. \tag{3}$$

In the above, Q_0 is the unloaded Q factor of the resonator, the main objective of the measurement

$$Q_0 = \frac{R_0}{\omega_0 L_0}. \tag{4}$$

III. Formation of a Loop on the Complex Plane

The second term on the right-hand side of (3) describes an exact circle on the complex impedance plane, when the frequency is varied. The addition of the linearly growing

Manuscript received June 16, 1983; revised February 23, 1984. This work was performed in the microwave laboratory of Harris Corporation, Farinon Division, in San Carlos.

Darko Kajfez is with the Department of Electrical Engineering, University of Mississippi, University, MS 38677.

Eugene Hwan is with Harris Corporation, Farinon Division, 1691 Bayport Avenue, San Carlos, CA 94070.

0018-9480/84/0700-0666$01.00 ©1984 IEEE

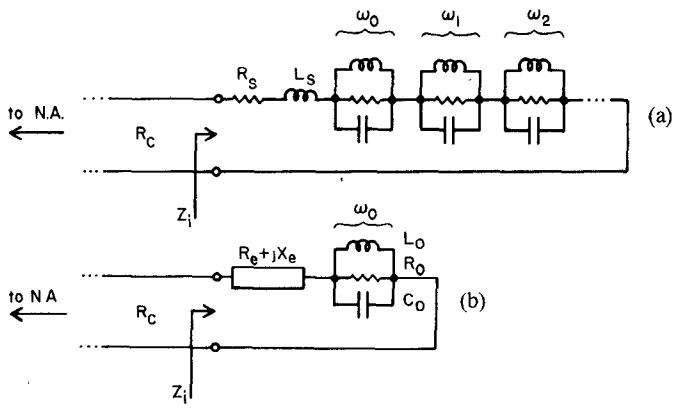

Fig. 1. (a) Complete equivalent circuit for the input impedance of an inductance-coupled cavity. (b) Simplified equivalent circuit for the vicinity of frequency ω_0. R_e can be neglected and X_e is a slowly varying reactance.

reactance X_e distorts the circle so that a loop is created on the complex plane Z_i. This will be demonstrated on a simple example of an inductance-coupled cavity. If the lowest resonant frequency ω_0 is considered, and if the presence of the higher resonant frequencies is neglected, the function X_e becomes

$$X_e = \omega_0 L_e(1+\delta) = X_1(1+\delta) \tag{5}$$

so that $2R_cQ_1 = X_1$. By taking a numerical example with $X_1 = 2R_c$, $R_0 = 1.5R_c$, and $Q_0 = 25$, the normalized input impedance is computed such as shown in Fig. 2. It is important to observe that the formation of a loop has similar effect, as if the Q-circle was shrunk. The apparently reduced circle no longer touches the imaginary axis. This fact may be wrongly interpreted as an indication that the coupling losses were present ($R_e \neq 0$). The application of the Ginzton's procedure for incorporating the effect of the coupling losses ([1], p. 424) would be a mistake in such a situation.

If the Q factor of one of the higher resonances was to be measured, the presence of the other resonant frequencies above and below the observed frequency would cause an increased slope Q_1 and the crossover point in Fig. 2 would move even farther away from the imaginary axis.

In the entire range of measured frequencies $\delta \ll 1$, so that the following approximation is valid:

$$\frac{\omega}{\omega_0} - \frac{\omega_0}{\omega} \simeq 2\delta. \tag{6}$$

The input impedance becomes

$$Z_i = j(X_1 + 2R_cQ_1\delta) + \frac{R_0}{1+j2Q_0\delta}. \tag{7}$$

It is easy to measure the two crossover frequencies on the impedance loop. Approximate computation can be made by assuming that $Q_0\delta \gg 1$, which leads to

$$\delta_{c0} = \pm\sqrt{\frac{R_0/R_c}{4Q_0Q_1}}. \tag{8}$$

The above expression is useful for estimating the slope Q_1 from the measured data, as explained later in Section V.

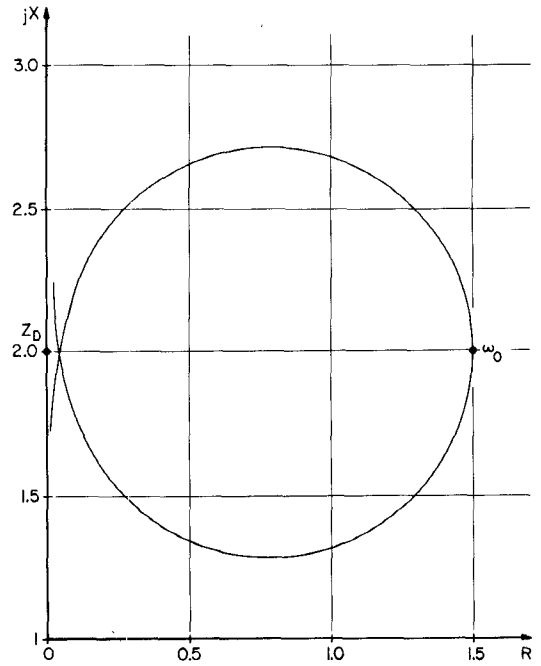

Fig. 2. Normalized input impedance Z_i for an inductance-coupled cavity.

The input reflection coefficient, displayed on the network analyzer, is

$$\Gamma_i = \frac{Z_i - R_c}{Z_i + R_c}. \tag{9}$$

The first term in (7) is slowly varying, and the second, resonant part is a fast varying function of δ. It is then convenient to introduce two functions, the slowly varying Z_s

$$Z_s = R_c\left[1 + j\left(\frac{X_1}{R_c} + 2Q_1\delta\right)\right] \tag{10}$$

and the fast varying Z_F

$$Z_F = \frac{R_0}{1+j2Q_0\delta}. \tag{11}$$

The input reflection coefficient then becomes

$$\Gamma_i = \frac{Z_F - Z_s^*}{Z_F + Z_s}. \tag{12}$$

If the coupling coefficient diminishes to zero, the input impedance at frequency ω_0 is given by the point Z_D on the imaginary axis (see Fig. 2). The corresponding reflection coefficient, for a decoupled resonator is

$$\Gamma_D = -\frac{Z_s^*}{Z_s}. \tag{13}$$

The difference $\Gamma_i - \Gamma_D$ takes a very simple form

$$\Gamma_i - \Gamma_D = \frac{2R_c}{Z_S^2\left(\frac{1}{Z_S} + \frac{1}{Z_F}\right)}. \tag{14}$$

The above expression is obtained without using any approximations. A simplification is possible due to the fact that $\delta \ll 1$ and $Q_1 \ll Q_0$. Denoting the normalized (con-

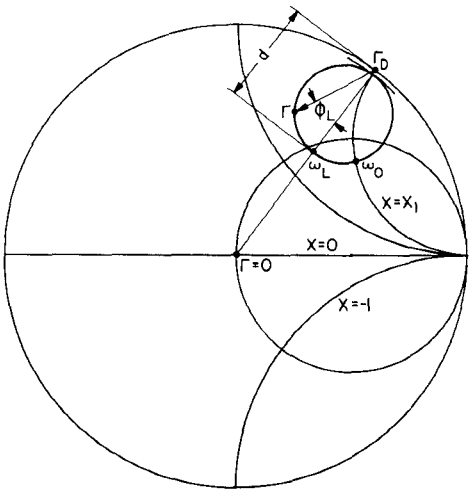

Fig. 3. Input reflection coefficient as a function of frequency.

stant) reactance by

$$x_1 = \frac{X_1}{R_c} \tag{15}$$

one can approximately express the term in parenthesis of (14) as follows:

$$\frac{1}{Z_s} + \frac{1}{Z_F} \simeq \frac{1}{R_c}\left(\frac{1}{1+x_1^2} + \frac{R_c}{R_0}\right)(1 + j2Q_L\delta_L). \tag{16}$$

In the above equation, the loaded detuning parameter is defined as

$$\delta_L = \frac{\omega - \omega_L}{\omega_0} = \delta - \frac{x_1\kappa}{2Q_0} \tag{17}$$

and the loaded Q factor is defined as

$$Q_L = \frac{Q_0}{1+\kappa} \tag{18}$$

while the coupling coefficient κ stands for

$$\kappa = \frac{R_0}{R_c(1+x_1^2)}. \tag{19}$$

Ginzton's definition of the coupling coefficient β is slightly different from the above definition

$$\beta = \frac{R_0}{R_c} = \kappa(1+x_1^2). \tag{20}$$

Equation (17) specifies the detuning due to coupling. Namely, when the input impedance from Fig. 2 is mapped onto a Smith chart, the loop still closely resembles a circle, as shown in Fig. 3. However, the magnitude of the reflection coefficient Γ_i is smallest at the frequency ω_L, which differs from the actual resonant frequency ω_0 of the unloaded resonator.

IV. Measurement of Q_0 via Q_L

By neglecting the δ dependence in (10), the following approximation is obtained for Z_s^2:

$$Z_s^2 \simeq R_c^2(1+x_1^2)e^{j2\tan^{-1}x_1}. \tag{21}$$

Then, (14) becomes

$$\Gamma_i - \Gamma_D = \frac{2e^{-j2\tan^{-1}x_1}}{\left(1+\frac{1}{\kappa}\right)(1+j2Q_L\delta_L)}. \tag{22}$$

The vector $\Gamma_i - \Gamma_D$ clearly describes a circle on a Smith chart. In the vicinity of frequency ω_L, the circle is a good approximation of the actual measured loop, but, when $Q_L\delta_L \gg 1$, the approximation breaks down. Therefore, for good accuracy, it is prudent to perform the measurement within the portion of the loop where $Q_L\delta_L \leq 1$. At $\omega = \omega_L$, the loaded detuning parameter $\delta_L = 0$, and the magnitude of the vector specified by (22) attains its maximum

$$|\Gamma_i - \Gamma_D|_{\max} = d = \frac{2}{1+\frac{1}{\kappa}}. \tag{23}$$

The value of d can be quite accurately measured on the Smith chart (see Fig. 3). Then, the coupling coefficient is computed from

$$\kappa = \frac{d}{2-d}. \tag{24}$$

It is to be noted that it was not necessary to assume $x_1^2 \ll 1$ in the above derivation. Even for moderate values of x_1, such as $x_1 = 2$, the relationship (24) is entirely valid.

The value of x_1 may be found from the Smith chart in Fig. 3 as being equal to the normalized reactance corresponding to the point Γ_D. If the reference plane for the impedance measurements is carefully established, the value of x_1 may be reliable, but a very small shift in the reference plane may considerably effect the value of x_1. Fortunately, x_1 is of secondary importance in the entire measurement, since it does not appear in (24).

The measurement of Q_L follows immediately from (22). As the frequency varies, the only variable in (22) is δ_L. The angle ϕ_L in Fig. 3 is then given by

$$\tan\phi_L = -2Q_L\delta_L. \tag{25}$$

At the center frequency ($f = f_L$), the angle ϕ_L is equal to zero. If one selects two frequencies f_3 and f_4 where $\phi_L = \pm 45°$, the loaded Q factor is found from (25), (17), and (2) as

$$Q_L = \frac{f_0}{f_3 - f_4} \approx \frac{f_L}{f_3 - f_4}. \tag{26}$$

If one wants to minimize possible error due to the fact that the loop locus differs from the idealized circle, he may select a smaller angle ϕ_L for measurement purposes. A convenient choice may be the angle 26.56°, which gives $\tan\phi_L = 0.5$. For an arbitrary choice of ϕ_L, the corresponding frequencies are denoted by f_1 and f_2. The formula for computation of Q_L is then

$$Q_L = \frac{f_L}{f_1 - f_2}\tan\phi_L. \tag{27}$$

Knowing Q_L and κ, one can then compute Q_0 from (18)

$$Q_0 = Q_L(1+\kappa). \tag{28}$$

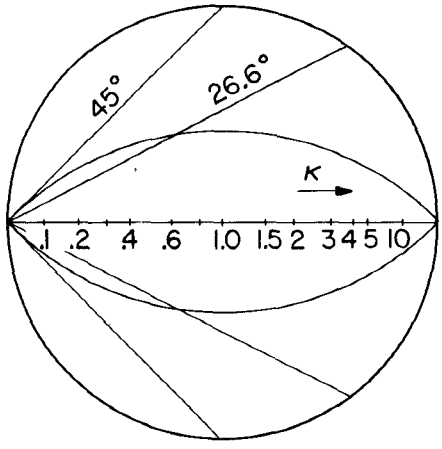

Fig. 4. Template for the polar display of the network analyzer.

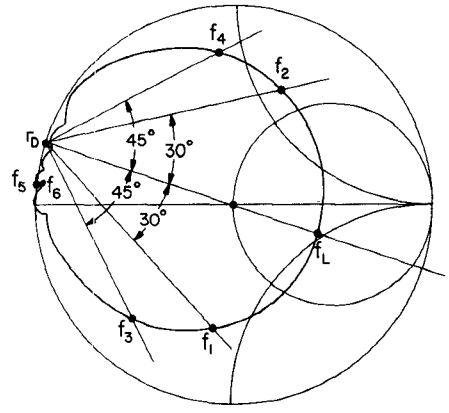

Fig. 5. Measured reflection coefficient of the resonator with coupling coefficient $\kappa = 2.64$

A transparent template is useful for reading the frequencies f_1 to f_4 on the polar display of the network analyzer. The template is shown in Fig. 4. If one is so inclined, he may engrave the scale for direct reading of κ as shown. The template is then rotated over the polar display until its center line coincides with Γ_D. Afterwards, the swept frequency operation is discontinued, and the accurate reading of the intersection frequencies is performed in "CW" operation with the aid of the frequency counter. Alternatively, if the frequency counter is not available, the network analyzer may be operated in a narrow swept range "ΔF", so that a circular arc is shown on the display. By adjusting the arc to extend to $\pm 45°$ points or to $\pm 26.56°$ points, the Q_L value can be computed in the same way as above. The frequency difference $f_1 - f_2$ or $f_3 - f_4$ can be read with sufficient accuracy directly from the "ΔF" scale on the network analyzer.

V. Example

To illustrate the procedure, consider the measurement of an inductance-coupled dielectric resonator. The measured input reflection coefficient in the swept frequency operation is shown in Fig. 5. The plot was made with an $x-y$ plotter attached to the output of the network analyzer, whereas the contours of the Smith chart and the lines for $\pm 45°$ and $\pm 30°$ were drawn later, with the help of reference points.

The frequencies for $\phi_L = \pm 45°$, measured with the microwave counter, were: $f_3 = 7.1730$ GHz, $f_4 = 7.1439$ GHz, and $f_L = 7.1575$ GHz. The measured diameter is $d = 1.45$, from which we complete the coupling $\kappa = 2.64$. Thus, $Q_L = 246$ and $Q_0 = 895$. Afterwards, the two frequencies at $\phi_L = \pm 30°$ were also measured. Their values were $f_1 = 7.1660$ GHz and $f_2 = 7.1491$ GHz, so that the corresponding $Q_L = 244$, in good agreement with the result obtained from the $\pm 45°$ lines.

From Fig. 5, it can be estimated that $x_1 = 0.16$. However, this value is not very reliable, because, in performing the measurement, the reference position on the transmission line leading to the network analyzer was not established with great care. With the use of (17), the resonant frequency of the decoupled resonator is then estimated to be $f_0 = 7.1406$ GHz. The crossover frequencies (end points in the swept measurement) were measured with a frequency counter to be $f_5 = 6.8575$ GHz and $f_6 = 7.3699$ GHz. Therefore, $2\delta_{c0} = 0.0716$, and from (8) and (19) we find the slope parameter of the external circuit

$$Q_1 = \frac{\kappa(1+x_1^2)}{Q_0(2\delta_{c0})^2} \tag{29}$$

which is here $Q_1 = 0.590$.

VI. Direct Measurement of Q_0

Q_0 can also be measured directly as follows: from (25), (23), and (18), one obtains

$$Q_0 = \frac{2\tan\phi_L}{(2-d)\delta_L}. \tag{30}$$

To find $2\delta_L$, which directly gives Q_0, one should require

$$\tan\phi_L = 1 - \frac{d}{2}. \tag{31}$$

This equation describes a circle of radius $\sqrt{2}$, passing through points Γ_d and $-\Gamma_d$.

Two such symmetrically positioned circles for direct reading of Q_0 can also be incorporated in the template as shown in Fig. 4. Again, it is to be noted that the above derivation is valid for nonvanishing values of x_1.

VII. Conclusion

The described measurement procedure consists of determining the "diameter" of the near-circular loop on the Smith chart and then measuring the frequency difference of two convenient points on the "circle." These points may be located at $\phi_L = \pm 45°$, $\pm 30°$, $\pm 26.65°$, or similar angles. In contrast with conventional procedure, it is not necessary to discriminate between the undercoupled and the overcoupled cases, because (24) covers both of them. Another distinction of the described procedure is that the frequency variation of the external reactance is not neglected, and an estimate of its slope Q_1 is obtained from the observation of the crossover point on the loop shown in the polar display of the network analyzer.

REFERENCES

[1] E. L. Ginzton, *Microwave Measurements*. New York: McGraw-Hill, 1957.

[2] S. F. Adam, *Microwave Theory and Applications*. Englewood Cliffs, NJ: Prentice-Hall, 1969.

[3] A. Khanna and Y. Garrault, "Determination of loaded, unloaded, and external quality factors of a dielectric resonator coupled to a microstrip line," *IEEE Trans. Microwave Theory Tech.*, vol. MTT-31, pp. 261–264, Mar. 1983.

[4] C. G. Montgomery, R. H. Dicke, and E. M. Purcell, *Principles of Microwave Circuits*. New York: Dover, 1965.

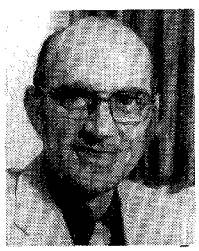

Darko Kajfez (SM'67) was born in Delnice, Yugoslavia, in 1928. He received the Dipl. Ing. degree in electrical engineering from the University of Ljubljana, Yugoslavia in 1953, and the Ph.D. degree from the University of California, Berkeley, in 1967.

Between 1950 and 1963, he worked with companies "Iskra" and "Rudi Cajavec" in Yugoslavia, primarily in the areas of microwave radios and radars. From 1963 to 1966, he was a research assistant at the Electronics Research Lab., University of California, Berkeley, investigating spiral and helical antennas for circular polarization, and their feeding circuits. In 1967, he joined the University of Mississippi, University, where he is presently Professor of Electrical Engineering. During the academic year 1976/77, he was a Visiting Professor at the School of Electrical Engineering, Ljubljana, Yugoslavia. His research and teaching interests are in the areas of electromagnetic theory and its applications to microwave circuits and antennas.

Eugene J. Hwan (S'65–M'65) received the Engineer's degree in 1960 from the Bandung Institute of Technology, Indonesia, and the M.S. degree in electrical engineering in 1966 from the University of California, Berkeley.

From 1960 to 1964, he worked at Siemens and Halske, Munich, Germany, in the field of communication systems. He was a Research Assistant at the Electronics Research Laboratory, University of California from 1965 to 1966. In 1966, he joined Aertech Industries working on microwave components and subsystems. Since 1973, he has been with the Farinon Division, Harris Corporation, where his responsibilities include development of frequency modulated oscillators, low-noise oscillators, and subsystems.

A Nonlinear Analysis of the Effects of Transient Electromagnetic Fields on Excitable Membranes

PAOLO BERNARDI, SENIOR MEMBER IEEE, AND GUGLIELMO D' INZEO, MEMBER, IEEE

Abstract—**The transmembrane voltage produced by a transient electromagnetic field has been determined using a nonlinear model of the cellular membrane. The influence on the membrane voltage of the various parameters characterizing the incident field, such as wave-shape, time-width, and amplitude, has been analyzed. In particular, the amplitude of the incident field for which the cell's behavior can be assumed as linear and the threshold level for exciting action potentials on the membrane have been determined. Potential hazards for humans exposed to transient fields are examined in light of this interaction mechanism.**

I. INTRODUCTION

THE EVALUATION of hazardous levels of nonionizing RF and microwave (MW) radiations requires a deep knowledge of the interaction mechanisms between electromagnetic (EM) fields and biological systems.

Manuscript received June 29, 1983; revised February 6, 1984.

The authors are with the Department of Electronics, University of Rome "La Sapienza," Italy.

The so-called thermal effect, produced by the energy dissipated within the tissue, has been, until now, the most examined one [1], [2]. Since the thermal effect is usually not influenced too much by the temporal behavior of the absorbed EM field, the major part of the literature on the subject is devoted to interactions produced by harmonic fields.

A nonthermal interaction mechanism, considered more recently [3]–[6], consists of the displacement of the membrane voltage from its resting value produced by the field acting at the cellular membrane level. This mechanism is strongly influenced by the temporal dependence of the field absorbed within the tissue. Therefore, it is important to analyze the effects produced on the membrane by EM fields having a general temporal behavior.

Mac Gregor [3], studying a linear model of the interaction process, has shown that a CW incident plane-wave with a frequency of 100 MHz and amplitude 200 V/m

0018-9480/84/0700-0670$01.00 ©1984 IEEE